
Article:
Saenphum, N., Chureemart, J., Evans, R. F.L. orcid.org/0000-0002-2378-8203 et al. (2 more authors) (2021) Large magnetoresistance in Heusler alloy-based current perpendicular to plane giant magnetoresistance sensors. Journal of Physics D: Applied Physics. 395004. ISSN 0022-3727

https://doi.org/10.1088/1361-6463/ac0ca4

Journal of Physics D: Applied Physics

Large magnetoresistance in Heusler alloy-based CPP-GMR Sensors

To cite this article before publication: Nattaya Saenphum *et al* 2021 *J. Phys. D: Appl. Phys.* in press https://doi.org/10.1088/1361-6463/ac0ca4

Large magnetoresistance in Heusler alloy-based CPP-GMR Sensors

N. Saenphum[1,2], J. Chureemart[1], R. F. L. Evans[3], R. W. Chantrell[3] and P. Chureemart[1,*]

[1] Department of Physics, Mahasarakham University, Mahasarakham, 44150, Thailand
[2] Seagate Technology, Teparuk, Samutprakarn, 10270, Thailand
[3] Department of Physics, University of York, York, YO10 5DD, United Kingdom

E-mail: phanwadee.c@msu.ac.th

Abstract. Increasing the data storage in next-generation hard disk drives requires a reduction in the physical dimensions of read sensors. Tunneling magnetoresistance (TMR) heads yield high magnetoresistance (MR) ratio but with a high resistance-area product (RA) that is suboptimal for devices. Giant magnetoresistance (GMR) head with different materials is an alternative way to improve reader performance with high MR ratio and low RA. In this paper, we theoretically study the effect of material properties and the layer thickness on RA and MR ratio in a trilayer system via an atomistic model combined with the spin transport model. The GMR stack can be constructed by the atomistic model and the RA and MR ratio can be directly calculated by considering the spin accumulation and spin current from the spin transport model. It is found that the spin valve using the Co_2FeAl Heusler alloy electrode with high spin polarization exhibits a high MR ratio and RA of 64 $m\Omega \cdot \mu m^2$ which is better than the spin valves using conventional ferromagnets (FM) such as Co, NiFe and CoFe. Moreover, we consider the thickness dependence of the change of RA (ΔRA). Increasing the free layer thickness yields the increase in ΔRA and MR ratio because of the enhancement of the bulk spin scattering. Additionally, the results show that the $\triangle$RA depends on the spin diffusion length of the nonmagnetic materials ($\lambda_{sdl,NM}$). The ΔRA increases from 3 up to 10 $m\Omega \cdot \mu m^2$ when $\lambda_{sdl,NM}$ increases from 35 to 1200 nm. This investigation shows the possibility for read head design of HDDs with areal density beyond 2 Tb/in^2.

1. Introduction

Magnetic data storage technology has been of interest and continually developed to increase the areal density (AD) or capacity of hard disk drives (HDDs) beyond 2 Tb/in^2. There are many proposed magnetic recording technologies to enable the next possibility to increase the amount of data bits stored in HDDs such as energy-assisted magnetic recording (EAMR) [1, 2, 3, 4, 5, 6] and bit patterned media recording (BPMR) [7, 8]. Although these magnetic recording technologies will allow the writing and storage of higher information densities, the readback of the information is equally challenging. Increases in data storage density can be achieved by scaling down characteristic dimensions. However, downward scaling of critical dimensions affects the functionality of all components of HDDs, critically including the sensors used to read back stored information. Nowadays, tunneling magnetoresistance (TMR) sensors have been widely used for read heads of HDDs due to their large magnetoresistance (MR) ratio. However, the intrinsically high resistance-area product (RA) due to the tunneling mechanism through the insulator barrier of TMR heads causes high noise and low data transfer rate. This leads to an intrinsic limitation of the TMR head for 2 Tb/in^2 HDD applications. Therefore, further improvement of read heads with a low RA and high MR output are crucial for the next stage in higher capacities, since a small RA results in high-speed reading performance [9, 10].

To alternatively achieve a high signal to noise ratio (SNR) and data transfer rate in next-generation HDD, a current perpendicular to plane giant magnetoresistance (CPP-GMR) is one of the promising candidates for magnetic recording head applications because it provides low RA compared with TMR read sensors [10, 11, 12]. However, the MR ratio of CPP-GMR sensor using conventional FM materials providing low spin polarization parameters [13, 14, 15] is still not high enough for read sensor applications. For further development in read heads with the minimum requirements of RA < 100 m$\Omega \cdot \mu$m^2 and MR ratio $> 20\%$ for HDDs with capacity beyond 2 Tb/in^2, a half-metallic ferromagnet (HMF) has been proposed as a promising candidate for read head applications. In order to enhance the change of resistance-area product (ΔRA) and the readback signal of the CPP-GMR read heads, the signal output is proportional to the spin-dependent scattering [16]. There are several theoretical [17, 18, 19, 20] and experimental [21, 22, 23, 24, 25] works reporting a high MR ratio of half-metallic Co-based Heusler alloys CPP-GMR. This is because the Heusler alloy provides a high spin polarization parameter resulting in a large spin-polarized current [26, 27, 28, 29, 30].

For next-generation reader designs, the effect of diffuse interfaces will become increasingly important with further scaling of device dimensions where the often-used micromagnetic model may be inappropriate. In this work, we therefore employ an advanced reader model at the atomistic level which can be handle the diffuse interface. It will be particularly used to investigate the transport property in Heusler alloy-based CPP-GMR sensors to meet the requirement of increasing AD in magnetic recording beyond the convention FM. The combination of atomistic model and the generalized spin accumulation model [31] is employed to study the effect of the FM material and layer thickness on the reader performance through the value of the resistance-area product and MR ratio. The former is used to model the stack of the reader and to observe the dynamics of magnetization whereas the latter is used to calculate the spatial MR by the value of spin accumulation and spin current. This study gives the new path and the possibility to develop the next generation reader with the requirement of high areal density and high read back signal. This also allows us to deeply understand the fundamental mechanism behind the operation of read head which is significantly beneficial in next-generation reader design.

2. Model description

A full understanding of the spin transport mechanism behind the reader sensors is significant for read head development. The atomistic model combined with the spin transport model implemented in the open source VAMPIRE software package [32] is employed to investigate the performance of read head. The atomistic model is first used to construct and observe the dynamic of magnetization in the spin valve stack comprising two FMs separated by a nonmagnetic (NM) layer. The spin transport behavior in a magnetic structure explained via the spin accumulation model strongly depends on the angle between magnetization in two FMs where their directions can be obtained from the atomistic model.

The atomistic model becomes necessary for spin valve construction and investigation of the magnetization profile in reader stack. Especially, for scaling down the dimension of reader, it allows us to deal with the diffuse interfaces which increasingly affect the MR behavior. The Landau-Lifshitz-Gilbert equation (LLG) in the presence of spin-transfer torque (STT) is employed to describe the

magnetization dynamics and is given by

$$\frac{\partial \mathbf{M}}{\partial t} = -\frac{\gamma}{(1+\alpha^2)}\mathbf{M}\times(\mathbf{B}_{\text{eff}}+J\mathbf{m}) - \frac{\gamma\alpha}{(1+\alpha^2)}[\mathbf{M}\times(\mathbf{M}\times(\mathbf{B}_{\text{eff}}+J\mathbf{m}))] \quad (1)$$

where $\mathbf{M}$ is the unit vector of the magnetization, $\mathbf{m}$ is the spin accumulation, γ is the gyromagnetic ratio, α is the damping constant and J is the $s-d$ exchange interaction constant. $\mathbf{B}_{\text{eff}} = \mu_0\mathbf{H}_{\text{eff}}$ is the effective field including the external applied field, the anisotropy field, the exchange field and the demagnetizing field [33].

To reduce the expensive computational cost, the macrocell approach is used to consider the demagnetizing field. The magnetic moment of the microcell can be determined from the summation of all spins in that cell. For all spins within the microcell i, the demagnetization field can be evaluated by the following equation,

$$\mathbf{B}_{\text{demag},i} = \frac{\mu_0}{4\pi}\sum_{j\neq i}\left[\frac{3(\vec{\mu}_j\cdot\hat{\mathbf{r}}_{ij})\hat{\mathbf{r}}_{ij}-\vec{\mu}_j}{|\vec{r}_{ij}|^3}\right] \quad (2)$$

and

$$\vec{\mu}_j = \mu_{\text{s}}\sum_{n=1}^{\text{n}_{\text{atom}}}\mathbf{S}_n \quad (3)$$

where μ_0 is the permeability of free space, $\vec{\mu}_j$ is the magnetic moment in the macrocell site j, $|\vec{r}_{ij}|$ and $\hat{\mathbf{r}}_{ij}$ are the distance and the unit vector between macrocell sites i and j respectively and n_{atom} denotes the number of atoms in the macrocell.

The effect of STT acting on the local magnetization can be represented as the additional field originated from the s-d exchange interaction of the magnetization with the spin accumulation ($\mathbf{m}$) [34, 35, 36, 37, 38]. STT contributed from the adiabatic and non-adiabatic torques can be considered from the spin accumulation and its magnitude strongly depends on the gradient of magnetization. In the rotated coordinate system where the local magnetization aligns in the direction of $\hat{\mathbf{b}}_1$, the solution of spin accumulation can be decomposed into two parts: the longitudinal ($\mathbf{m}_\parallel$) and transverse ($\mathbf{m}_\perp$) components which can be expressed as follows [35, 38],

$$\begin{aligned}\mathbf{m}_\parallel(x) &= \left[m_\parallel(\infty)+\left[m_\parallel(0)-m_\parallel(\infty)\right]e^{-x/\lambda_{\text{sdl}}}\right]\hat{\mathbf{b}}_1\\ \mathbf{m}_{\perp,2}(x) &= 2e^{-k_1x}[u\cos(k_2x)-v\sin(k_2x)]\hat{\mathbf{b}}_2\\ \mathbf{m}_{\perp,3}(x) &= 2e^{-k_1x}[u\sin(k_2x)+v\cos(k_2x)]\hat{\mathbf{b}}_3,\end{aligned} \quad (4)$$

with

$$(k_1\pm ik_2) = \sqrt{\lambda_{\text{sf}}^{-2}\pm i\lambda_J^{-2}}$$

where λ_{sdl} is the spin diffusion length, the spin-flip length is defined as $\lambda_{\text{sf}} = \sqrt{2D_0\tau_{sf}}$ and λ_{J} is the spin-precession length. The unknown coefficients u, v and $m_\parallel(0)$ can be determined by assuming that the spin current constantly flows across the interface. The spin current ($\mathbf{j}_m$) at any position along the direction of electron flow is given by,

$$\mathbf{j}_m(x) = \beta j_e\mathbf{M} - 2D_0\left[\frac{\partial\mathbf{m}}{\partial x}-\beta\beta'\mathbf{M}\left(\mathbf{M}\cdot\frac{\partial\mathbf{m}}{\partial x}\right)\right], \quad (5)$$

where β and β' are the spin polarization parameters of the material, j_e is the charge current density and D_0 is the diffusion constant.

The involvement of layer-wise discretization of the magnetic system and the self-consistent solutions of the magnetization and the spin accumulation is used for the GMR calculation. To determine the performance of the reader via the value of RA and the MR ratio, the spatial resistance-area product (RA_i) can be considered from the relationship between the spin current (j_m) and the rate of change of spin accumulation (Δm) given by [39, 40]

$$RA_i = \frac{|\Delta m|\text{V}_{\text{cell}}\text{k}_\text{B}\text{T}}{j_m e^2}, \quad (6)$$

where V_{cell} is the microcell volume, j_m is the spin current and e is the electron charge. The value of $\text{k}_\text{B}\text{T}$ used here [41, 31] is 10 meV or 1.6×10^{-21} J. Subsequently, the total RA of the system is calculated by summing the resistance of all microcells, $RA = \sum_{i=1}^{n} RA_i$ where n is the number of microcells. Consequently, the MR ratio can be considered, $\%\text{MR} = \frac{|\text{R}_\text{P}-\text{R}_\text{AP}|}{\text{R}_\text{P}}$.

3. Results and discussions

In this paper, we aim to develop and design an appropriate read sensor for next-generation HDDs. As is well known, the GMR strongly depends on the contribution of bulk and interfacial spin scattering. This indicates that choosing a suitable ferromagnet used as the sensing layer in the reader stack is important. Therefore, we first investigate the influence of magnetic properties of different FM materials on the CPP-GMR performance in the trilayer system of Co(5nm)/Cu(5nm)/FMs(5nm) where FMs are Co, NiFe, CoFe, Co_2FeAl (CFA), Co_2FeSi (CFS) and $Co_2FeAl_{0.5}Si_{0.5}$(CFAS) by employing the atomistic model combined with the spin transport model. The transport parameters of these candidate ferromagnets at 0 Kelvin are shown in Tab. 1. It is noted that the investigation of temperature effect is not studied here.

Table 1. Transport Properties of selected ferromagnetic materials at 0 K

Materials	β	β'	λ_{sdl} (nm)	m_∞ (MC/m^3)	Refs.
Co	0.50	0.90	60	39.45	[31]
CoFe	0.56	0.73	12	261.50	[42, 43]
NiFe	0.70	0.95	5	111.80	[31]
CFA	0.99	0.86	3	6.80	[21, 44]
CFS	0.86	0.96	1.7	15.71	[44]
CFAS	0.92	0.85	3	3.09	[45, 44]

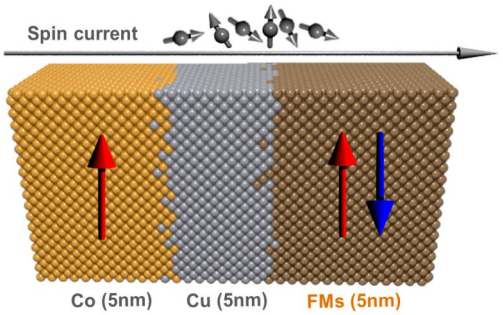

Figure 1. (Color online) The trilayer system of Co(5nm)/Cu(5nm)/FMs(5nm): The red and blue arrows represent the magnetization in the direction of $\pm y$, respectively.

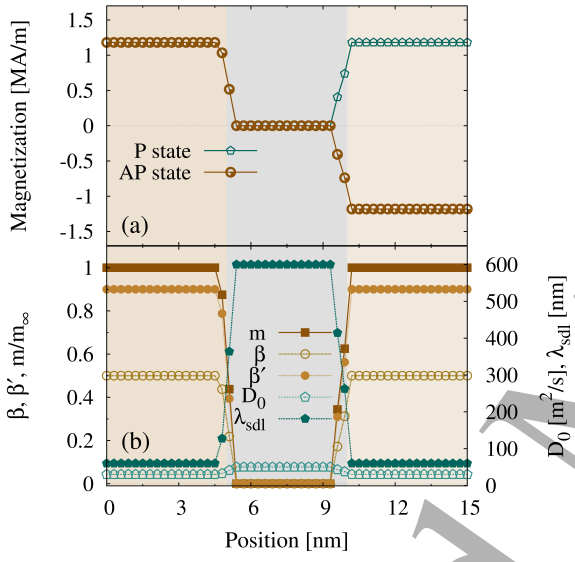

Figure 2. (Color online) The magnetization and transport parameters at any position of Co(5nm)/Cu(5nm)/Co(5nm) structure with the diffuse interface of 1 nm

We first construct the reader stack including the diffuse interfaces by using the atomistic model. The spin transport behavior in the junction of the real device is regulated by the interfacial roughness between the ferromagnet and the nonmagnet. To make for more practical assessment, the density of spin species close to the interface is represented by an interfacial mixing which can arise during the sputtering process. This can be modelled via a probability distribution (P) given by,

$$P = \frac{1}{2}[-\tanh(\frac{x - x_0}{D}) + 1] \quad (7)$$

where x is any given position of the structure, x_0 is the center position of the interface and D is the atomic diffuse constant associated with the interface thickness. The magnetization of the free layer is considered in two configurations (P and AP states) whereas that of pinned layer is fixed in the y direction as demonstrated in Fig. 1.

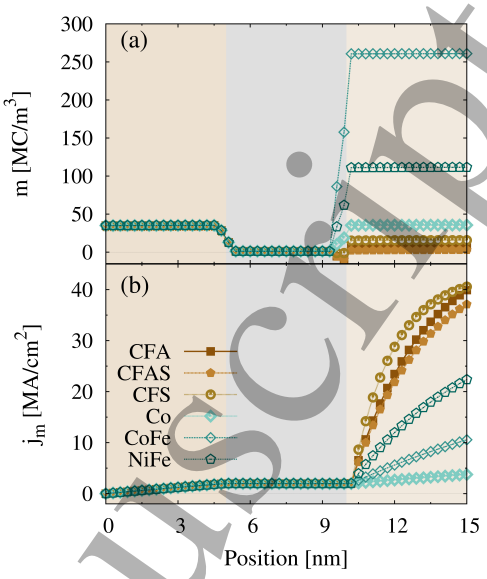

Figure 3. (Color online) (a) The spin accumulation and (b) the spin current at any position of the Co/Cu/FMs system with parallel state comparing different free layer materials. The results show that the spin accumulation and spin current strongly depend on the spin diffusion length and spin polarization of the free layer material.

The variation of transport parameters at any position can be determined by averaging transport parameter values of all atoms. This results in spatially varying magnetization and the spin transport parameters across the interface as shown in Fig. 2. The behavior of spin transport in the reader stack can be observed by injecting a charge current with a density of 50 MA/cm^2 into the system.

Subsequently, the time and position dependence of spin accumulation and spin current of both configurations can be evaluated by using Eqs. (4) and (5). As a result of the P state in Fig.3, it clearly demonstrates that the s-d exchange interaction results in the alignment of spin current and spin accumulation in the direction of the magnetization. The spin accumulation is likely to reach its equilibrium value (m_∞) whereas the spin current can be fully polarized over the distance of the spin diffusion length. We observe the discontinuity of spin accumulation across the FM/NM interface because the transport properties of these two materials are different. This eventually leads to a high interfacial spin-dependent scattering. Furthermore, the spin accumulation gradually decreases from the value at the Co/Cu interface ($x = 5$ nm) close to zero which is the equilibrium value of spin accumulation of Cu. It is important to note that the Cu layer should be thin enough which is much less than λ_{sdl} of Cu to conserve the spin polarized current and to decouple the interaction between two ferromagnets. The results demonstrate that both spin accumulation and spin current are relatively unchanged in the Cu layer.

At the second interface of Cu/FM, the rapid change in

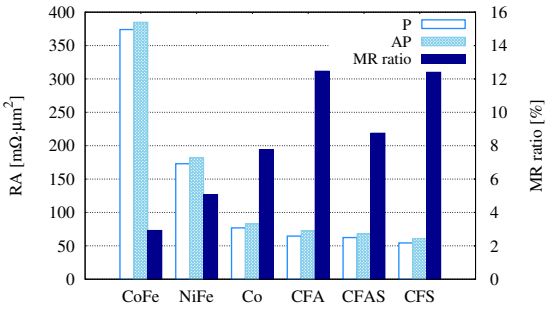

Figure 4. (Color online) RA of parallel and anti-parallel states ar MR ratio of Co(5nm)/Cu(5nm)/FMs(5nm) structure with different fr layer materials. The Heusler alloy materials show a significant advantage compared with the conventional ferromagnetic systems.

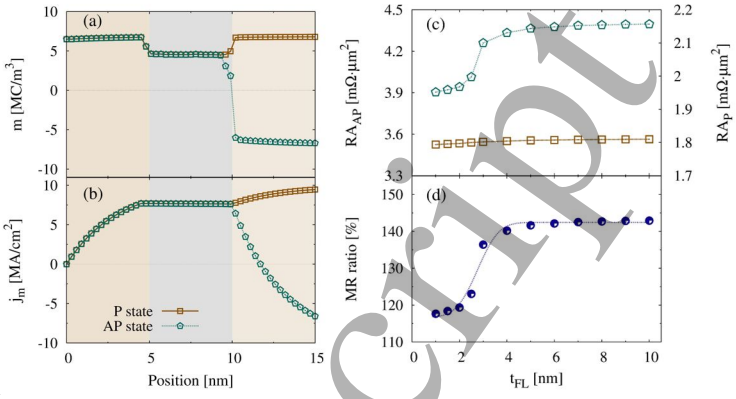

Figure 5. (Color online) The position dependence of (a) the spin accumulation and (b) the spin current of the CFA/Cu/CFA with parallel and anti-parallel states. The free layer thickness dependence of (c) RA in parallel and anti-parallel states and (d) MR ratio. The dot line is a guide to the eyes.

spin accumulation is obviously seen in the case of Co, CoFe and NiFe. For Heusler alloys with high spin polarization parameters, the spin current can be easily polarized in the direction of the local magnetization compared with that in conventional FMs as demonstrated in Fig. 3(b). Especially in CFS, the spin current can be fully polarized fastest with the length scale of $\lambda_{sdl} = 1.7$ nm. To consider the promising materials for CPP-GMR sensors, the resistance-area product of both P and AP states are directly determined from the spatial spin accumulation and spin current as shown in Eq. (6) and the MR ratio is subsequently evaluated. As seen in Fig 4, it is found that the CPP-GMR using the typical FM materials as the free layer gives high RA and low MR ratio due to the rapid change in spin accumulation at the interface (high Δm) and low spin polarized current. In contrast, the CPP-GMR structure with CFA, CFS and CFAS Heusler alloy materials yield low RA of 64, 62 and 54 $m\Omega \cdot \mu m^2$, respectively which meet the requirement for the next-generation of HDDs with low RA $< 100\ m\Omega \cdot \mu m^2$. In addition, the result indicates that higher spin polarized current eventually gives rise to higher MR ratio in CPP-GMR sensors with half-metallic Co-based Heusler alloys. The MR ratio in CPP-GMR with CFAS and CFA were found to be larger than the other ferromagnetic materials. Our results are in agreement with previous experiments showing the inversely proportional relationship between the magnetoresistance and the spin polarization of the material [46, 22, 21, 47]. The Heusler alloys materials could therefore be a good candidate for next generation read sensors.

To increase the areal density of HDDs by reducing the grain size in the recording media, this subsequently leads to the reduction in size of the read element. Typically, the size of the read sensor should be less than twice as big as the data bit length. The thickness of the free (sensing) and spacer layers become significant factor in the readback process to avoid noise arising from neighbour bits. Therefore, the next investigation of interest is the film thickness dependence of the MR ratio representing the difference in readback signal of P and AP states. A charge current density of 10 MA/cm^2 is injected perpendicularly to the plane of the CFA(5nm)/Cu(5nm)/CFA(t_{FL}) structure where the free layer thickness (t_{FL}) is varied from 1 to 10 nm. The spatial variation of the spin accumulation and spin current are demonstrated in Fig. 5 (a) and (b) respectively. They are likely to orient in the direction of the magnetization as expected. The change in the spin accumulation at the interface make a major contribution on the enhancement of the RA value, especially for the anti-parallel configuration. As demonstrated in Fig. 5 (c), the RA for the parallel configuration is fairly constant with increasing FL thickness. On the other hand, the RA value of the anti-parallel configuration increases with increasing FL thickness and becomes saturated for a thickness of $t_F > 5$ nm. Increasing layer thickness increases the contribution of bulk spin scattering and the spin current becomes fully polarized. However, saturation of RA is appeared when the layer thickness is larger than the spin diffusion length of CFA ($\lambda_{sdl} = 3$ nm). Consequently, the result in Fig. 5 (d) shows the trend of MR ratio which is similar to the RA_{AP}. This indicates the thickness dependence of RA and MR ratio. Our results give the same trend as experimental measurements [45, 48, 49, 50].

To optimize the reader size to achieve a high MR ratio, the thickness of the FL should be comparable to the λ_{sdl} of the material. In addition, the property of the nonmagnet used as the spacer layer becomes a significant factor affecting the spin transport behavior and performance of the reader. To complete the investigation for reader design, we finally study the dependence of the MR ratio on the spacer thickness ranging from 1-5 nm in the structure of CFA(5nm)/Cu(t_{NM})/CFA(5nm). The spacer layer is inserted in the reader stack to remove the exchange coupling between two ferromagnets. Its thickness should be appropriate to avoid this exchange coupling and to

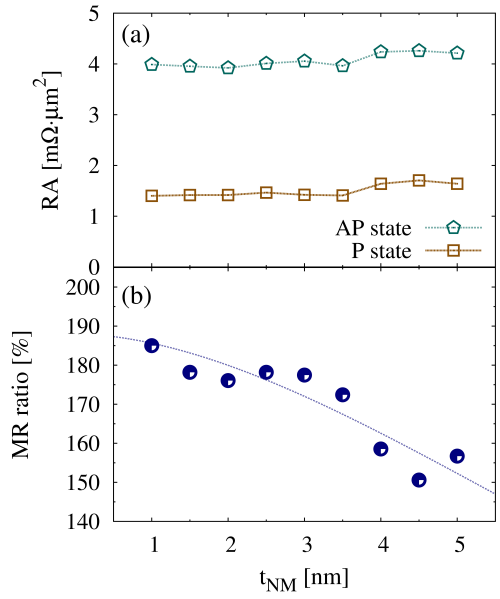

Figure 6. (Color online) The thickness dependence of (a) RA in the CFA/Cu/CFA structure with P and AP states and (b) MR ratio

conserve the direction of spin polarized current. As shown in Fig. 6, it is found that the RA of both P and AP states is slightly sensitive to the spacer thickness. However, it can be observed that the MR ratio is strongly affected by the spacer thickness. This indicates the reduction in the spin transport efficiency through the spacer layer. The trend of the calculated MR and MR ratio is consistent with previous reports [51, 52]. Our results clearly reveal that a high output signal from the read head can be achieved by optimizing the thickness of the free and spacer layers. Our results show the possibility to develop next generation readers with the requirement of high AD and also allows us to deeply understand the fundamental mechanisms behind the operation of read sensors which is highly beneficial in next-generation reader design.

4. Conclusions

In conclusion, we investigate the effect of crucial factors on the performance of the CPP-GMR reader to maximize the value of the MR ratio. As a consequence of the reduction in device sizes, the interface property becomes an important factor determining device functionality and performance. The combination of the atomistic model and the spin accumulation model provides a state-of-the-art model of read head devices including atomistic details such as intermixing, roughness and defects. The MR and MR ratio are determined from the spin current and the rate of change of spin accumulation. Firstly, we considered promising materials for the development of next-generation reader by investigating spin transport in the trilayer system of FM/NM/FM with different FMs. Our results show that the MR ratio depends on the type and spin transport properties of the material as well as the film thicknesses. The MR ratio is likely to increase with increasing spin polarization parameter. We found that the spin valve structure with Heusler alloys (Co_2FeAl) providing high spin polarization results in low RA and high MR ratio. Moreover, we observe the thickness dependence of spin transport behavior and found that the GMR values increase with increasing free layer thickness and saturate at a certain thickness, $t_{FL} > \lambda_{sdl}$. It also shows that the MR output was degraded with increasing of a spacer thickness consistent with experiments. The model can be applicable for device design to consider an appropriate FM material used in reader stack and to optimize a layer thickness to obtain high performance reader with low RA and high MR output.

Acknowledgment

P.C. and J. C. gratefully acknowledge the funding from Mahasarakham University and National Research Council of Thailand (NRCT) under Grant No. NRCT5-RSA63014.

[1] D. Weller et al., IEEE transactions on magnetics **50**, 1 (2013).
[2] C. Vogler, C. Abert, F. Bruckner, D. Suess, and D. Praetorius, Applied Physics Letters **108**, 102406 (2016).
[3] C. Vogler, C. Abert, F. Bruckner, D. Suess, and D. Praetorius, Journal of Applied Physics **119**, 223903 (2016).
[4] S. Okamoto, N. Kikuchi, M. Furuta, O. Kitakami, and T. Shimatsu, Journal of Physics D: Applied Physics **48**, 353001 (2015).
[5] J.-G. Zhu and Y. Wang, IEEE Transactions on Magnetics **46**, 751 (2010).
[6] Z. Liu, P.-W. Huang, S. Hernandez, G. Ju, and T. Rausch, IEEE Transactions on Magnetics **54**, 1 (2018).
[7] T. R. Albrecht et al., IEEE Transactions on Magnetics **49**, 773 (2013).
[8] T. R. Albrecht et al., IEEE Transactions on Magnetics **51**, 1 (2015).
[9] K. Nagasaka, Journal of Magnetism and Magnetic Materials **321**, 508 (2009).
[10] M. Takagishi, K. Yamada, H. Iwasaki, H. N. Fuke, and S. Hashimoto, IEEE Transactions on Magnetics **46**, 2086 (2010).
[11] A. Hirohata et al., IEEE Transactions on Magnetics **51**, 1 (2015).
[12] A. Hirohata, W. Frost, M. Samiepour, and J.-y. Kim, Materials **11**, 105 (2018).
[13] T. Nakatani et al., IEEE Transactions on Magnetics **48**, 1751 (2012).
[14] S. Wurmehl et al., Applied Physics Letters **98**, 012506 (2011).
[15] T. Kimura, N. Hashimoto, S. Yamada, M. Miyao, and K. Hamaya, NPG asia materials **4**, e9 (2012).
[16] T. Valet and A. Fert, Physical Review B **48**, 7099 (1993).
[17] N. Strelkov, A. Vedyaev, and B. Dieny, Journal of applied physics **94**, 3278 (2003).
[18] N. Chung, M. B. Jalil, S. Tan, and S. Bala Kumar, Journal of Applied Physics **103**, 07F308 (2008).
[19] V. Prudnikov, P. Prudnikov, and D. Romanovskiy, Journal of Physics D: Applied Physics **49**, 235002 (2016).
[20] T. Taniguchi, H. Imamura, T. M. Nakatani, and K. Hono, Applied Physics Letters **98**, 042503 (2011).
[21] T. Furubayashi et al., Journal of Applied Physics **114**, 123910 (2013).
[22] H. Goripati, T. Furubayashi, Y. Takahashi, and K. Hono, Journal of Applied Physics **113**, 043901 (2013).
[23] T. Kubota, Y. Ina, Z. Wen, H. Narisawa, and K. Takanashi, Physical Review Materials **1**, 044402 (2017).
[24] S. Li et al., AIP Advances **8**, 075230 (2018).

[25] G. Zahnd et al., Scientific reports **7**, 9553 (2017).
[26] S. Idrissi, S. Ziti, H. Labrim, and L. Bahmad, Multidiscipline Modeling in Materials and Structures **17**, 552 (2020).
[27] S. Idrissi, H. Labrim, S. Ziti, and L. Bahmad, Physics Letters A **384**, 126453 (2020).
[28] S. Idrissi, H. Labrim, S. Ziti, and L. Bahmad, Solid State Communications **331**, 114292 (2021).
[29] S. Idrissi, S. Ziti, H. Labrim, and L. Bahmad, Chinese Journal of Physics **70**, 312 (2021).
[30] S. Idrissi, S. Ziti, H. Labrim, and L. Bahmad, Journal of Low Temperature Physics **202**, 343 (2021).
[31] P. Chureemart, R. Cuadrado, I. D'Amico, and R. Chantrell, Physical Review B **87**, 195310 (2013).
[32] R. F. L. Evans et al., Journal of Physics: Condensed Matter **26**, 103202 (2014).
[33] R. F. Evans et al., Journal of Physics: Condensed Matter **26**, 103202 (2014).
[34] S. Zhang, P. M. Levy, and A. Fert, Phys. Rev. Lett. **88**, 236601 (2002).
[35] P. Chureemart, I. D'Amico, and R. Chantrell, Journal of Physics: Condensed Matter **27**, 146004 (2015).
[36] P. Chureemart, R. F. L. Evans, I. D'Amico, and R. W. Chantrell, Phys. Rev. B **92**, 054434 (2015).
[37] C. Petitjean, D. Luc, and X. Waintal, Phys. Rev. Lett. **109**, 117204 (2012).
[38] N. Saenphum, J. Chureemart, R. Chantrell, and P. Chureemart, Journal of Magnetism and Magnetic Materials **484**, 238 (2019).
[39] A. Fert and H. Jaffres, Physical Review B **64**, 184420 (2001).
[40] N. Saenphum, J. Chureemart, R. Chantrell, and P. Chureemart, Journal of Magnetism and Magnetic Materials **484**, 238 (2019).
[41] J. Chureemart, R. Cuadrado, P. Chureemart, and R. Chantrell, Journal of Magnetism and Magnetic Materials **443**, 287 (2017).
[42] H. Yuasa et al., Journal of applied physics **92**, 2646 (2002).
[43] T. Hamada, T. Ohno, and S. Maekawa, Molecular Physics **113**, 314 (2015).
[44] H.-L. Huang, J.-C. Tung, and G.-Y. Guo, Physical Review B **91**, 134409 (2015).
[45] T. Nakatani et al., Applied Physics Letters **96**, 212501 (2010).
[46] S. Li et al., AIP Advances **8**, 075230 (2018).
[47] S. Oki et al., Applied Physics Express **5**, 063004 (2012).
[48] T. Nakatani, T. Furubayashi, and K. Hono, Journal of Applied Physics **109**, 07B724 (2011).
[49] K. Nikolaev et al., Applied Physics Letters **94**, 222501 (2009).
[50] T. Nakatani et al., Scripta Materialia **189**, 63 (2020).
[51] J. C. Read et al., Journal of Applied Physics **118**, 043907 (2015).
[52] S. Li et al., Journal of Applied Physics **119**, 093911 (2016).